Detecting local synchronization in coupled chaotic systems

L. Pastur, S. Boccaletti, and P. L. Ramazza
Istituto Nazionale di Ottica Applicata, Largo Enrico Fermi 6, 50125 Florence, Italy
(Received 24 March 2003; published 4 March 2004)

We introduce a technique to detect and quantify local functional dependencies between coupled chaotic systems. The method estimates the fraction of locally synchronized configurations, in a pair of signals with an arbitrary state of global synchronization. Application to a pair of interacting Rössler oscillators shows that our method is able to quantify the number of dynamical configurations where a local prediction task is possible, as well as in the absence of global synchronization features.

DOI: 10.1103/PhysRevE.69.036201 PACS number(s): 05.45.Xt, 05.45.Ac, 05.45.Tp

In the past, much attention has been devoted to characterizing coupled chaotic systems exhibiting synchronization regimes [1]. In this framework, different synchronization features have been studied, such as, e.g., identical and generalized synchronization [2,3], phase synchronization [4], and lag and intermittent lag synchronization [5]. Furthermore, synchronization effects have been explored in natural phenomena [6], and controlled laboratory experiments [7].

In this context, various attempts to provide unifying definitions for encompassing the different synchronization phenomena have been pursued [8]. Recently, a formal approach to the problem has been put forward [9], in which the unifying property of synchronization is established in the emergence of local functional dependencies between neighborhoods of particular phase space configurations in the projected spaces of the two coupled subsystems. The approach assumes a system $\mathbf{Z} \in \mathbb{R}^{m_1+m_2}$ divisible into two coupled subsystems, $\mathbf{X} \in \mathbb{R}^{m_1}$ and $\mathbf{Y} \in \mathbb{R}^{m_2}$. In this framework, synchronization is equivalent to predictability of one subsystem's values from another, i.e., that an event $\tilde{y}$ in $\mathbf{Y}$ always occurs when a particular event $\tilde{x}$ in $\mathbf{X}$ occurs. However, when searching for evidence of synchronization in data, one seldom has data that fall right on a given $\tilde{x}$ or on a given $\tilde{y}$. Rather, the closer $x(t)$ is to $\tilde{x}$ the closer $y(t)$ is to $\tilde{y}$. The latter statement is captured rigorously by a local *continuous* function; namely, the trajectories of $x(t)$ close to $\tilde{x}$ are mapped near to $\tilde{y}$ by a local function that is continuous at the point $(\tilde{x},\tilde{y})$, and that, near $(\tilde{x},\tilde{y})$ describes well the predictability of subsystem $\mathbf{Y}$ dynamics from subsystem $\mathbf{X}$ dynamics. Reference [9] gives a general, formal mathematical ground to the above statements, and establishes the sufficient conditions for a system to display global synchronization features, i.e., to admit local functional dependencies regardless on the particular choice of the $(\tilde{x},\tilde{y})$ phase space configuration.

For a generic pair of coupled chaotic systems, however, it is to be expected that synchronization occurs only at some locations (if any) of the phase space, and not globally. In this case, a continuous functional dependence of $y(t)$ on $x(t)$ will exist only locally around a set of synchronization points $\{\tilde{x}_s,\tilde{y}_s\}$.

Implementation of a search for local functional dependencies requires two separate steps: a preliminary one in which the two interacting subsystems $\mathbf{X}$ and $\mathbf{Y}$ are properly identified within the original dynamical systems $\mathbf{Z}$, with their dimensionalities measured, and a second one in which the local synchronization points $(\tilde{x},\tilde{y})$ are detected. The first problem was solved recently in Ref. [10] by means of a modification of the *false nearest neighbors* algorithm [11], allowing for a separate measurement of the dimensionalities of weakly coupled systems in the case of emergent synchronization motions.

In this paper, we will address the second step of the search by introducing the *synchronization points percentage* (SPP) indicator, and show how one can gather information on local synchronization properties emerging in coupled chaotic systems.

We start by assuming to have N data points in $\mathbf{Z} \in \mathbb{R}^{m_1+m_2}$. By means of a proper subspace reconstruction [10], we end up with N data points in $\mathbf{X} \in \mathbb{R}^{m_1}$ and N corresponding images in $\mathbf{Y} \in \mathbb{R}^{m_2}$. We then pick a specific point $\tilde{x} \in \mathbf{X}$ and consider its image $\tilde{y} \in \mathbf{Y}$.

The first task consists of identifying proper domains and co-domains for a statistical analysis of the existence of functional dependency. For this purpose, we choose a pair of positive real numbers (ε_k,δ) (the index k being an integer), and consider the volume $U_{\varepsilon_k} \subset \mathbf{X} (V_\delta \subset \mathbf{Y})$ containing all points whose m_1 distance (m_2 distance) from $\tilde{x}$ ($\tilde{y}$) is smaller than ε_k (δ). Furthermore, we look at all points in $\mathbf{X}$ falling within U_{ε_k}, and verify the imaging condition, that is, we ask ourselves whether or not all images of the points in U_{ε_k} fall within V_δ. If the answer is no, we choose $\varepsilon_{k+1} < \varepsilon_k$, and repeat the above procedure. If for all k the imaging condition is not satisfied, the task ends with the conclusion that no local functional dependency exists in the vicinity of the chosen configuration $(\tilde{x},\tilde{y})$. If, instead, for a given $\tilde{k}$ the imaging condition is verified, the task ends with the identification of a valid pair $(\varepsilon_{\tilde{k}},\delta)$, over which one has to test for the existence of a continuous functional relationship.

Figure 1 helps in understanding the schematic representation of the procedure. In the following we will denote with $U \subset \mathbf{X}$ $(V \subset \mathbf{Y})$ the neighborhood $U_{\varepsilon_{\tilde{k}}}$ (V_δ) surrounding $\tilde{x}(\tilde{y})$, and assume that $m < N$ points fall within U. By construction, the number of points falling within V will be $n \geqslant m$, reflecting the fact that V might host also images of points not belonging to U.

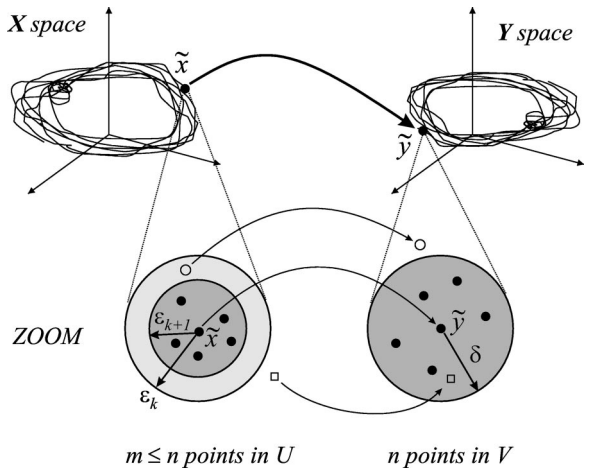

FIG. 1. Schematic representation of the statistical continuity analysis. The upper part shows the reconstructed trajectories in the two subspaces **X** and **Y**, and the location of the points $\tilde{x}$ and $\tilde{y}$. The lower part zooms in on the U,V neighborhoods. For $\varepsilon=\varepsilon_{k+1}$, V contains all images of the m points in U (solid circles), plus images of other points (empty squares) from outside U. For $\varepsilon=\varepsilon_k$, some points in U (empty circles) have images outside V.

The probability of a single point falling within V is $P(V)\equiv n/N$, and the probability that m points fall within V by pure chance is $P_m(V)=P(V)^m=(n/N)^m$. This latter quantity, for reasonable choices of n,m [reasonable pairs $(\varepsilon_{\tilde{k}},\delta)$], is a very small number. However, one has to fix a *confidence level* of comparison, for assessing existence of a local continuous function between the two neighborhoods. This problem was addressed in Ref. [12], where the *continuity statistics* method was proposed. This consists of calculating the quantity b_P, defined as

$$b_P=\max_{q=1,\ldots,m} B(q,m;P), \tag{1}$$

where $B(q,m;P)$ is the binomial distribution, giving the probability that $q\leqslant m$ events out of m attempts are realized for a process of elementary probability P.

As said above, the presence of a single data within V has probability $P(V)$. The quantity b_P [for $P=P(V)$] represents then the maximum over q of the probability that, given m points, q out of them fall into V. Hence a level of confidence for the existence of a continuous function can be estimated in terms of the ratio

$$\Theta=\frac{P_m(V)}{b_P}. \tag{2}$$

If $\Theta\approx 1$ we have no trustable information about the existence of such a functional relationship, insofar as the chance probability of having our m points in V is of the same order of the maximum probability of having events in V out of m attempts. On the contrary, if $\Theta\ll 1$, the chance probability of having our m points in V is negligible compared to b_P. Thus one concludes that the two sets U and V are the domain and co-domain, respectively, of a local continuous function mapping states in **X** close to $\tilde{x}$ to states in **Y** close to $\tilde{y}$. This answers the practical question of predicting states in **Y** with error δ from measurements of states in **X** with error $\varepsilon_{\tilde{k}}$.

We have made use of the original formulation of the continuity statistics [12], that explicitly considers $P=P(V)$ in Eq. (2). More recently, the authors of Ref. [12] have proposed an alternative way for measuring the confidence level, by choosing $P=1/2$ in the denominator of Eq. (2), corresponding to a hypothesis of equal probability for an attempt to fall within or outside the selected box [13].

Our technique for characterizing synchronization consists then of the three following points: (i) check the imaging of neighborhoods of a given configuration $\tilde{x}$ into neighborhoods of $\tilde{y}$; (ii) assess the degree of confidence that such an imaging process comes from the existence of a local continuous function; (iii) repeat points (i) and (ii) for all N pairs of configurations $(\tilde{x},\tilde{y})$ available in the data set. This procedure allows a classification of the different dynamical states into locally synchronized and nonsynchronized ones. As a result one can introduce the synchronization points percentage (SPP) indicator, as the ratio between the total number $\tilde{n}$ of locally synchronized configurations and the total number of available points N.

The proposed method can be applied to any kind of multivariate data set, for the detection of hidden local synchronization properties, that cannot be detected by global indicators, such as correlation functions, Lyapunov exponents, Lyapunov functionals, or any other kind of time (or ensemble) average indicators that unavoidably result in mixing locally synchronized and unsynchronized configurations. As a result, the SPP indicator furnishes relevant information in all those cases in which synchronization states emerge locally in phase space, to detect predictability properties that are limited to some subset of the dynamics.

In order to illustrate the robustness of the method, in the following we will refer to a test case, represented by a pair of nonidentical bidirectionally coupled chaotic Rössler oscillators. Here $m_1=m_2=3$, and the subspaces **X** and **Y** contain state vectors $\mathbf{x}\equiv(x_1,y_1,z_1)$ and $\mathbf{y}\equiv(x_2,y_2,z_2)$ whose evolution is ruled by

$$\begin{aligned}
\dot{x}_{1,2}&=-\omega_{1,2}y_{1,2}-z_{1,2}+\epsilon(x_{2,1}-x_{1,2}),\\
\dot{y}_{1,2}&=\omega_{1,2}x_{1,2}+0.165z_{1,2},\\
\dot{z}_{1,2}&=0.2+z_{1,2}(x_{1,2}-10).
\end{aligned} \tag{3}$$

In Eqs. (3), $\omega_{1,2}=\omega_0\pm\Delta$ represent the natural frequencies of the two chaotic oscillators, $\omega_0=0.97$, $\Delta=0.02$ is the frequency mismatch, and $\epsilon>0$ rules the coupling strength. As ϵ increases, the emergence of different synchronization features in Eqs. (3) has been described and characterized in the literature [4,5]. Precisely, for $\epsilon<0.036$ no global synchronization (NS) is established, in terms of the global indicators proposed up to now. For $0.036\leqslant\epsilon\leqslant 0.11$ a phase synchronized (PS) regime emerges characterized by the boundedness in time of the phase difference $\Delta\phi\equiv|\phi_1-\phi_2|$[$\phi_{1,2}\equiv\arctan(y_{1,2}/x_{1,2})$ being the phases of the two oscillators], whereas the two chaotic amplitudes remain almost uncorre-

lated [4]. At larger coupling strengths ($\epsilon \geqslant 0.145$), lag synchronization (LS) is established, corresponding to a collective motion wherein $|\mathbf{x}(t)-\mathbf{y}(t-\tau)|$ is bounded over the whole dynamical evolution ($\tau>0$ represents here a lag time) [5]. In this regime, increasing ϵ results in gradually decreasing τ, eventually ending with a regime indistinguishable from complete synchronization (CS).

Most of the transition points between these regimes were also identified in Ref. [5], by inspection of the Lyapunov spectrum of Eqs. (3) as a function of the coupling strength. Precisely, the NS to PS (PS to LS) transition occurs for that value of ϵ for which a previously zero (positive) Lyapunov exponent becomes negative. On the other hand, the LS to CS transition is a smooth transition that can be tracked by use of the time averaged similarity function [5]. In the following we apply our method with a threshold value of $\Theta=0.1$ for the discrimination of whether or not the coupled systems display local functional relationships.

An intermediate synchronization regime between PS and LS exists in the range $0.11 \leqslant \epsilon < 0.145$, called intermittent lag synchronization (ILS), where the system (3) displays long epochs of LS evolution, interrupted by persistent bursts of desynchronized motion. This has been observed numerically, and put in relation with the system's trajectory passing through configurations where one globally negative Lyapunov exponent has a local positive value. Since ILS is an intimately local phenomenon, its transition point has not been captured by those techniques that measure time or ensemble averaged quantities. As a result, up to now, studies on ILS have been limited to numerical investigations [5], or based upon the role in the synchronization process played by the different unstable periodic orbits visited by the dynamics [14]. We will show that our SPP indicator is able to discriminate between ILS and PS regimes, as well as to directly identify the PS to ILS transition point.

We have performed long time simulations of Eqs. (3) at several coupling strength values, and collected data points from the two scalar outputs x_1 and x_2. For each ϵ, data points are collected over a time corresponding to 1.7×10^5 Rössler cycles, with a sampling frequency of ten points per cycle. Simulations were performed with a standard fourth order Runge-Kutta method, and with random initial conditions. Furthermore, the standard embedding technique [15] was used to reconstruct the three dimensional vector states $\mathbf{x}$ and $\mathbf{y}$ from time-delayed coordinates of the scalar variables x_1 and x_2, and calculation of the SPP indicator was performed on the reconstructed spaces.

Figure 2 reports the behavior of the SPP indicator vs the coupling strength ϵ, calculated by fixing δ so as $n=150$ points are falling within V. Fixing n results in general in an error δ that is not constant over the attractor. On the other side, if the measure is strongly nonhomogeneous, fixing δ could generate situations in which n is so small that the statistics becomes meaningless. These concerns do not apply, however, in the case of the Rössler system for the parameters used in Eqs. (3), since the density of points is roughly homogeneous over the attractor and both choices lead

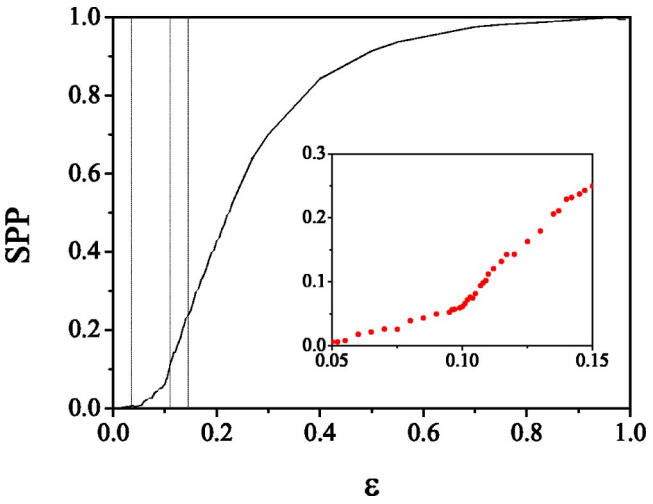

FIG. 2. SPP indicator (see text for definition) vs coupling strength ϵ. The vertical dashed lines indicate the transition points between the different synchronization regimes. The inset shows a zoom limited to the range $0.05<\epsilon<0.15$, where the PS to ILS transition point is located at $\epsilon_c \simeq 0.10$. Notice the two different slopes in the linear growth of SPP for $\epsilon<\epsilon_c$ and $\epsilon>\epsilon_c$.

to equivalent results. As one expects, SPP increases monotonically as the coupling strength increases, saturating to 1 when approaching the CS regime.

Interesting information can be extracted by inspection of SPP within those synchronization regimes, such as PS and ILS that do not correspond to global synchronization features. In particular, it is found that SPP is linearly increasing with ϵ in both regimes, but with two different slopes (see the inset of Fig. 2). The linear increase of the indicator already within PS is a relevant result. Indeed, if and to which extent PS implies weak correlations in the chaotic amplitudes was

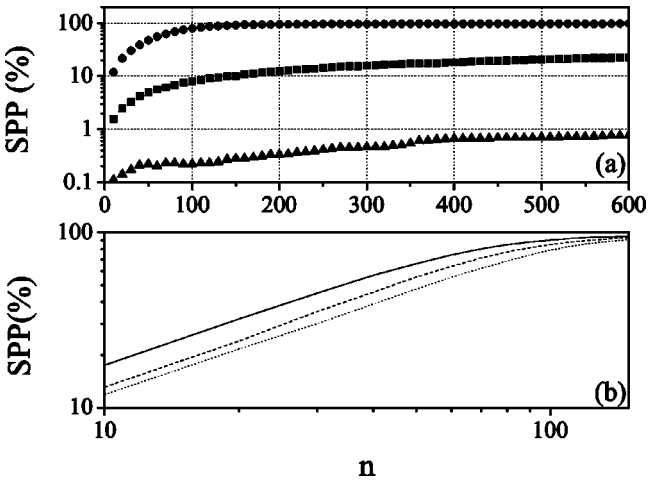

FIG. 3. (a) SPP indicator vs number n of points falling within V for $\epsilon=0.01$ (triangles, NS), $\epsilon=0.08$ (squares, PS), and $\epsilon=0.155$ (circles, LS). (b) SPP vs n within the LS regime for $\epsilon=0.155$ (dotted line), $\epsilon=0.17$ (dashed line), and $\epsilon=0.19$ (continuous line). For all cases, before saturation ($n \leqslant 50$), SPP depends on n with a scaling law SPP $\sim n^{\beta}$ with $\beta \sim 0.85$. For $n>50$ the three curves saturate to 100% of synchronization points.

yet unknown, and constituted an issue generating controversy. The present result shows that PS does imply an increasing percentage of local functional relationship, thus quantifying directly the degree of amplitude synchronization within such a regime. Furthermore, the crossover point between the slopes of the two linear growths allows one to identify the PS to ILS transition point at $\epsilon \simeq 0.10$, that none of the various indicators used in previous works was capable to reveal.

Finally, other interesting information can be extracted from the scaling behavior of SPP with n, that is with enlarging the radius δ of the image box in the **Y** subspace. Figure 3(a) shows SPP vs n for the NS, PS, and LS regimes. In all cases, the SPP indicator increases monotonically. For LS (circles) it fastly saturates to 1 (the same value as CS). This is reflecting the fact that LS differs from CS only due to the presence of a lag time τ. Enlarging too much the neighborhood size results in V to fully overlap with all images of points in U shifted by a phase factor $\omega\tau$, where ω is the mean frequency of the oscillator, thus making indistinguishable LS from CS.

More insights on this property can be extracted from Fig. 3(b), where SPP is reported vs n within the LS regime for different values of ϵ, corresponding to different values of the lag time τ. Here one sees that, before saturation, SPP depends on n with a scaling law SPP $\sim n^{\beta}$ with a unique exponent $\beta \sim 0.85$ for the three ϵ values. However, the three curves saturate to 1 at three different values of n, reflecting the behavior of τ within LS, that monotonically decreases as ϵ increases.

Coming again to Fig. 3(a), one realizes that for both NS (triangles) and PS (squares), the SPP indicator is always bounded away from 1. This indicates that in these regimes a global predictability of one subsystem's states from measurement in the other subspace is never possible for any choice of resolution. However, given a resolution δ in the image subspace (a maximum error allowed in the prediction), our indicator quantifies the number of states that can be locally predicted at that resolution, thus revealing that local hidden synchronization features can be extracted for prediction purposes, also in those cases in which global dependencies are not established. This feature might be relevant for detecting configurations where a local prediction can be assessed, in many situations where a global prediction procedure fails.

In real data, the effect of noise is to reduce the resolution in the phase space, so that the statistics relative to boxes containing a small number of points is not reliable anymore. A threshold in n should therefore be introduced, typically corresponding to δ's larger than the noise-induced uncertainty.

The authors are indebted to L. Moniz and L. M. Pecora for many fruitful discussions. This work was partially supported by EU Contract No. HPRN-CT-2000-00158, and MIUR Project No. FIRB n. RBNE01CW3M_001. L.P. acknowledges support from Contract No. MCFI-2000-01822.

[1] For an overview of this matter, we direct the reader to A. Pikovsky, M. Rosenblum, and J. Kurths, *Synchronization: A Universal Concept in Nonlinear Sciences* (Cambridge University Press, Cambridge, England, 2001); S. Boccaletti, J. Kurths, G. Osipov, D. Valladares, and C. Zhou, Phys. Rep. **366**, 1 (2002).

[2] H. Fujisaka and T. Yamada, Prog. Theor. Phys. **69**, 32 (1983); L.M. Pecora and T.L. Carroll, Phys. Rev. Lett. **64**, 821 (1990).

[3] N.F. Rulkov, M.M. Sushchik, L.S. Tsimring, and H.D.I. Abarbanel, Phys. Rev. E **51**, 980 (1995); L. Kocarev and U. Parlitz, Phys. Rev. Lett. **76**, 1816 (1996).

[4] M.G. Rosenblum, A.S. Pikovsky, and J. Kurths, Phys. Rev. Lett. **76**, 1804 (1996).

[5] M.G. Rosenblum, A.S. Pikovsky, and J. Kurths, Phys. Rev. Lett. **78**, 4193 (1997); S. Boccaletti and D.L. Valladares, Phys. Rev. E **62**, 7497 (2000).

[6] C. Schafer, M.G. Rosemblum, J. Kurths, and H.H. Abel, Nature (London) **392**, 239 (1998); P. Tass, M.G. Rosemblum, M.G. Weule, J. Kurths, A. Pikovsky, J. Volkmann, A. Schnitzler, and H.J. Freund, Phys. Rev. Lett. **81**, 3291 (1998); G.D. Van Wiggeren and R. Roy, Science **279**, 1198 (1998); A. Neiman, X. Pei, D. Russell, W. Wojtenek, L. Wilkens, F. Moss, H.A. Braun, M.T. Huber, and K. Voigt, Phys. Rev. Lett. **82**, 660 (1999); G.M. Hall, S. Bahar, and D.J. Gauthier, *ibid.* **82**, 2995 (1999); B. Blasius, A. Huppert, and L. Stone, Nature (London) **399**, 354 (1999); D.J. DeShazer, R. Breban, E. Ott, and R. Roy, Phys. Rev. Lett. **87**, 044101 (2001).

[7] C.M. Ticos, E. Rosa, Jr., W.B. Pardo, J.A. Walkenstein, and M. Monti, Phys. Rev. Lett. **85**, 2929 (2000); D. Maza, A. Vallone, H. Mancini, and S. Boccaletti, *ibid.* **85**, 5567 (2000); E. Allaria, F.T. Arecchi, A. Di Garbo, and R. Meucci, *ibid.* **86**, 791 (2001).

[8] I.I. Blekhman, A.L. Fradkov, H. Nijmeijer, and A.Yu. Pogromsky, Syst. Control Lett. **31**, 299 (1997); R. Brown and L. Kocarev, Chaos **10**, 344 (2000).

[9] S. Boccaletti, Louis M. Pecora, and A. Pelaez, Phys. Rev. E **63**, 066219 (2001).

[10] S. Boccaletti, D.L. Valladares, L.M. Pecora, H.P. Geffert, and T. Carroll, Phys. Rev. E **65**, 035204 (2002).

[11] M.B. Kennel, R. Brown, and H.D.I. Abarbanel, Phys. Rev. A **45**, 3403 (1992); H.D.I. Abarbanel, *Analysis of Observed Chaotic Data* (Springer-Verlag, New York, 1996).

[12] L. Pecora, T. Caroll, and J. Heagy, Phys. Rev. E **52**, 3420 (1995).

[13] L. Moniz and L. M. Pecora (private communication).

[14] D. Pazó, M.A. Zaks, and J. Kurths, Chaos **13**, 309 (2003).

[15] F. Takens, in *Detecting Strange Attractors in Turbulence*, edited by D.A. Rand and L.S. Young, Lecture Notes in Mathematics Vol. 898 (Springer-Verlag, New York, 1981); T. Sauer, M. Casdagli, and J.A. Yorke, J. Stat. Phys. **65**, 579 (1991).